doi:10.4028/www.scientific.net/MSF.794-796.278

# Effect of cold plastic deformation prior to ageing on creep resistance of an Al-Cu-Mg-Ag alloy

Marat Gazizov[a *], Ivan Zuiko[b] and Rustam Kaibyshev[c]

Laboratory of Mechanical Properties of Nanostructured Materials and Superalloys, Belgorod State University, Pobeda 85, Belgorod, 308015, Russia

[a]gazizov@bsu.edu.ru, [b]zuiko_ivan@bsu.edu.ru, [c]rustam_kaibyshev@bsu.edu.ru

* corresponding author

**Keywords:** Aluminum alloys; Cold working; Precipitation; Microstructure; Mechanical properties.

**Abstract.** Effect of thermomechanical processing on creep resistance at 150°C of an Al-5.6Cu-0.72Mg-0.5Ag-0.32Mn-0.17Sc-0.12Zr (wt. %) alloy was examined. It was shown that increasing strain prior to artificial aging provides achieving high strength. However, a degradation of the creep resistance, i.e., significant decrease in the rupture time and increase in the minimal creep rate, took place, concurrently. The effect of cold rolling on the strength and creep resistance is discussed in relation with the strain effect on the dispersion of secondary phases. The increase in strength and degradation of creep properties of the alloy subjected to cold working before ageing result from superposition of two competitive processes. First, an increase in the lattice dislocation density facilitates the precipitation of Ω-phase plates with high aspect ratio, leading to increase in the static strength at room temperature. Second, acceleration of the diffusion processes results in coarsening of strengthening phase in grain/subgrain interiors and precipitation of Ω-phase on deformation-induced boundaries during creep that deteriorates creep resistance.

## Introduction

The aluminum alloys belonging to Al-Cu-Mg-Ag system exhibit excellent mechanical properties at room and elevated temperatures that make it possible to consider them as a material for use in aerospace engineering for structures operating at elevated temperatures [1-3]. The excellent mechanical properties of Al-Cu-Mg-Ag alloys result from the formation of a fine and uniform dispersion of hexagonal-shaped plate-like Ω-phase ($Al_2Cu$) precipitates on the $\{111\}_{Al}$ matrix planes, which is promoted by Ag addition to the alloy with high Cu/Mg ratios, during artificial aging. Heterogeneous nucleation of semicoherent particles of θ'-phase ($Al_2Cu$) on dislocations competes with the precipitations of Ω plates and may deteriorate creep resistance of Al-Cu-Mg-Ag alloys, although appearance of imperceptible fraction of θ'-phase plates aligned along $\{001\}_{Al}$ matrix planes does not affect the creep resistance remarkably.

Thermomechanical processing (TMP) of these alloys includes solution treatment, quenching in water, cold stretching or/and rolling to a strain of 4-10% and subsequent artificial ageing [1,4,5]. However, the effect of the cold strain on the static mechanical properties and creep resistance of Al-Cu-Mg-Ag alloys has not been sufficiently investigated. There is a potential for additional increase in the strength owing to the formation of stable subgrain structure by plastic deformation. Thereby, the aim of this paper is to investigate the effect of cold deformation prior to ageing on the mechanical properties of an Al-Cu-Mg-Ag alloy at room and elevated temperatures.

## Experimental details

An aluminum alloy with a chemical composition of Al-5.6Cu-0.72Mg-0.5Ag-0.32Mn-0.17Sc-0.12Zr-0.1Ge (wt %) was prepared by semi-continuous casting. Initially, ingots with dimensions of ∅40 mm×120 mm were subjected to a two-step homogenization annealing at 360°C for 6 h,

followed by subsequent heating to 510°C and soaking for 24 h [6,7]. Next, the ingots were forged at 400°C with a forging ratio of 4:1 to produce rectangular billets. Rods with dimensions of 20 mm×20 mm×100 mm were machined from these billets parallel to the major axis. These rods were solution treated at 525°C for 1 h followed by water quenching.

The specimens for tension were prepared from parts of solution treated rods and then tensioned with strain ranging from 1 to 10%. Other parts of solution treated rods were cold rolled with reductions of 20, 40 and 80%. For attaining the peak ageing condition the cold deformed samples were immediately aged at 190°C for 2h.

Flat specimens for tensile and creep testing had dog-bone shape with the gauge length of 25 mm, the width of 7 mm and the thickness of 3 mm for all test conditions. They were cut from the central part of the rolled samples with flat surface parallel to the major ingot axis or rolling plane. The tensile tests were carried out at room temperature at a constant rate of crosshead displacement, with initial strain rate of $1.3\times10^{-3}$ $s^{-1}$. Computer-controlled ATS Lever Arm Testers, model #2330, with WinCCS II Software equipped three zone furnace were used for the creep tests at 150°C with applied stress ranging from 270 MPa to 360 MPa.

The specimens for microstructural characterization were prepared from gauge length sections parallel to the major axis or RD. The microstructures were examined using a JEOL JEM-2100 transmission electron microscope (TEM) with accelerating potential of 200 kV in bright field (BF) mode. The TEM specimens were electropolished at 20 V in a solution of 30%-$HNO_3$ and 70%-$CH_3OH$ at a temperature of -30°C using a Tenupol-5 twin-jet polishing unit.

The apparent diameter (D) and thickness (h) of each second phase particle were measured from BF-TEM images with the electron beam orientated parallel to the $<011>_{Al}$ zone axis of the matrix. About 200-300 measurements were carried out for each data point.

## Results and discussion

Table 1 Effect of cold deformation and ageing at 190°C for 2 h on the tensile properties

| Treatment | YS [MPa] | UTS [MPa] | Elongation to failure [%] |
|---|---|---|---|
| Solution treatment | 145 | 370 | 22 |
| Ageing (190°C, 2 h | 450 | 495 | 8.9 |
| 1% + ageing (190°C, 2 h) | 440 | 485 | 8.6 |
| 3% + ageing (190°C, 2 h) | 460 | 495 | 8.4 |
| 5% + ageing (190°C, 2 h) | 465 | 495 | 7.7 |
| 7% + ageing (190°C, 2 h) | 480 | 515 | 7.4 |
| 10% + ageing (190°C, 2 h) | 480 | 510 | 6.8 |
| 20% + ageing (190°C, 2 h) | 505 | 530 | 6.5 |
| 40% + ageing (190°C, 2 h) | 530 | 560 | 6.1 |
| 80% + ageing (190°C, 2 h) | 535 | 570 | 5.9 |

The nature, average size, shape and distribution of the secondary phases in the alloy were previously described in detail [6,7]. The microstructure of the solution treated alloy consisted of initial grains having average dimensions of ~48 and ~30 μm in the longitudinal and transverse directions, respectively. Coarse particles of the primary θ-phase and ternary W-phase ($Al_{8-x}Cu_{4+x}Sc$) were situated on grain boundaries [6,7]. It is worth noting that the coherent particles of the $Al_3(Sc,Zr)$ phase having average size of ~25 nm were non-uniformly distributed within interiors of grains [6,7].

The maximal ageing response of the experimental alloy after cold deformation to strains ranging from 0 to 80% was obtained at 190°C for 2 h. The results of tensile tests are summarized in Table 1. The yield stress (YS) of 450 MPa, ultimate tensile strength (UTS) of 495 MPa with elongation to failure of ~9% can be achieved in present alloy without prior cold deformation [8]. An increase of the cold strain leads to gradual increase of the YS and UTS values. The alloy subjected to cold rolling with a reduction of 80% demonstrates the highest YS and UTS of ~535 MPa and ~570 MPa, respectively, and the lowest elongation-to-failure of ~6% [8].

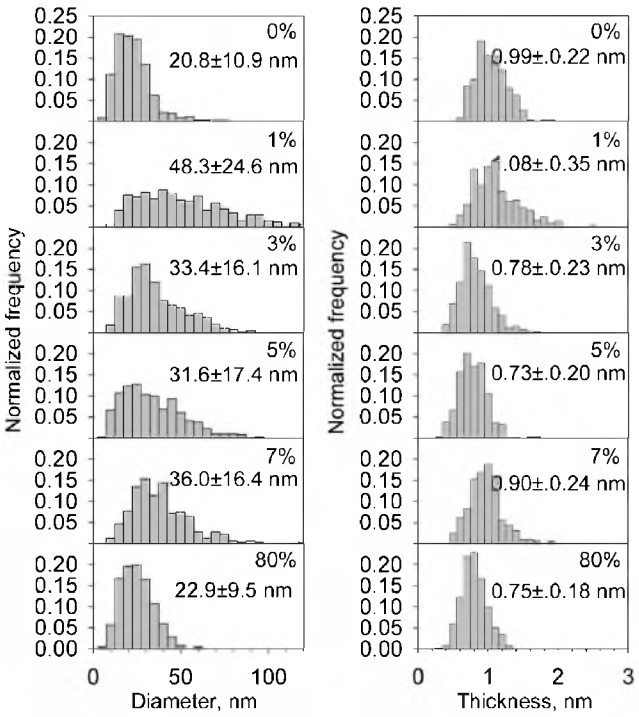


Fig. 1 Effect of prior deformation on dimensions of the Ω-phase plates within grains/subgrains interiors after ageing at 190°C, 2h.

Analysis of the microstructure after cold deformation to different strains and ageing at 190°C for 2 h does not reveal changes in the morphology of the predominant Ω-phase particles in grain/subgrain interiors (Fig. 1). The particle aspect ratio (AR) (diameter/thickness) increases from 20 to 40 with increase in the cold strain to 3% due to increase in diameter, mainly, and remains unchanged in the samples strained to 3-7%. The lowest plate thickness of ~0.75 nm was observed at strains of 5 and 80%. This can lead to significant increase of increment in critical resolved shear stress (CRSS) due to interfacial strengthening and/or order strengthening [9]. The Orowan strengthening cannot be considered as operative because the estimated values of its increments are significantly higher than the strength values of the processed samples [8]. The AR value decreased to 28 at ε~80%.

It should be noted that the Ω-phase plates situated on the deformation induced boundaries are significantly thicker (~4 nm) than the particles in the grain/subgrain interiors. A negligible increase in the density of θ′-phase particles was also observed due to the fact that cold deformation prior to ageing increased the nucleation sites for this phase.

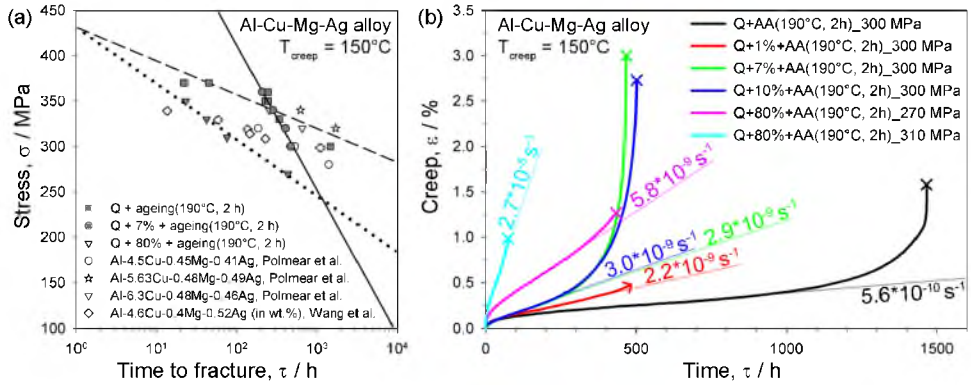


Fig. 2 Dependences of rupture time vs applied stress [1,4,10] (a) and creep curves at nearly the same level of applied stresses (b) for samples subjected to different TMPs.

Fig. 2a shows the dependences of rupture time vs applied stress at 150°C for samples subjected to strains of 0%, 7%, 80%. Relevant data of creep tests for other Al-Cu-Mg-Ag alloys after TMPs involving cold deformation to strains of 0-1% [1,4,10] are also presented for comparison. The creep curves at nearly the same level of applied stresses for the samples after different TMPs are shown in Fig. 2b. In general, the creep resistance tends to decrease with increasing prior cold strain. The linear extrapolation of these experimental data in Fig. 2a shows that there is a strong effect of the intermediate strain followed by aging on creep resistance. High rupture time and low minimal creep rates were demonstrated by the sample after treatment without cold deformation. Intermediate deformation deteriorates the creep properties. The cold strains of 7 to 10% decrease the rupture time by a factor of about 3 and increase the minimal creep rate by a factor of about 5 (Fig. 2b). Extensive cold rolling highly deteriorates the creep resistance (Fig. 2). Moreover, duration of tertiary creep for samples after cold rolling with a reduction of 80% followed by ageing is significantly shorter as

compared with samples deformed to strains ranging from 0 to 10%. It is worth noting that elongation-to-failure under creep conditions is lower by factors of about 2 or 3 in comparison with tensile test.

The microstructures of gage regions and the distribution of diameter and thickness of Ω-phase within grains/subgrains in the ruptured specimens after creep test are presented in Fig. 3 and 4, respectively. The plates of Ω-phase tend to grow under creep inhomogeneously that leads to appearance of a bimodal-like distribution of their dimensions (Fig. 4). There is significant number of Ω-phase plates with thickness more than 2 nm and, therefore, the transverse boundaries of these particles lost coherency with aluminum matrix and became semi-coherent [8]. The fraction of thicker Ω plates is higher as compared with samples before test [8] (Fig. 3c). It is worth noting that the finer Ω plates are observed in sample after prior cold rolling to 80% followed by ageing creep at 150°C. It seems that this fact results from redistribution of alloying elements between strengthening precipitates situated within grains/subgrains and on grain/subgrain boundaries. The AR of the Ω-phase plates of ~28 does not depend on the applied stress.

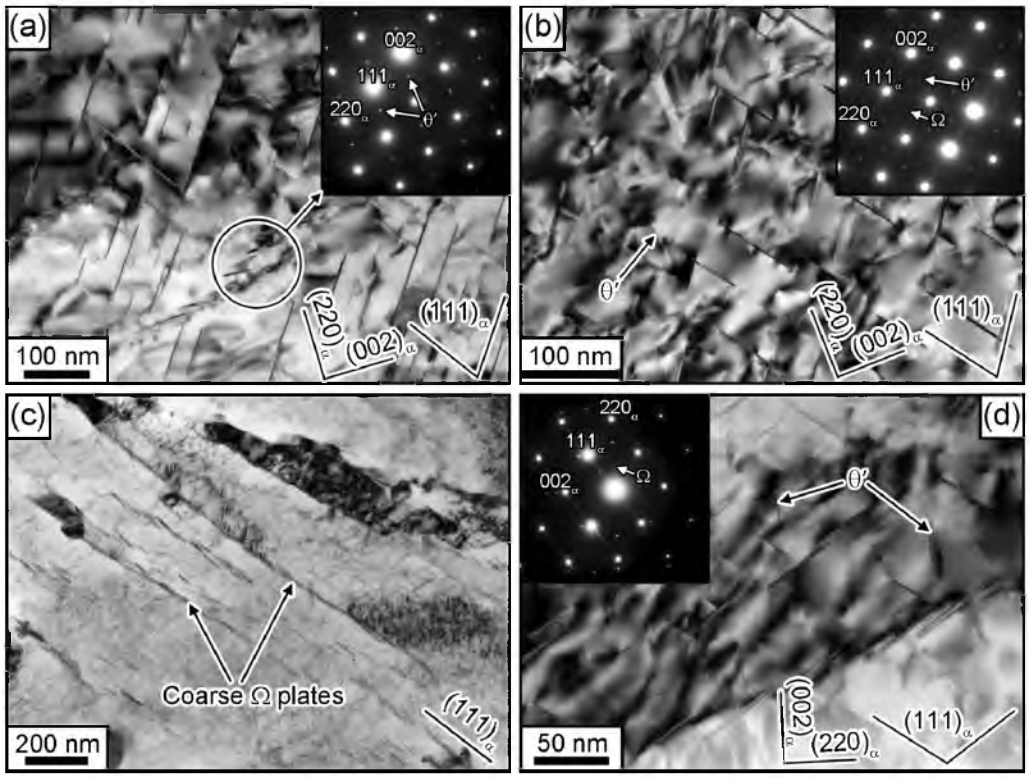


Fig. 3 Microstructure of gage regions of samples after creep test to fracture at 150°C. Initial treatments: (a) quenching + ageing (190°C, 2 h), (b) tensioned (7%) + ageing (190°C, 2 h), (c) cold rolling (80%) + ageing (190°C, 2 h).

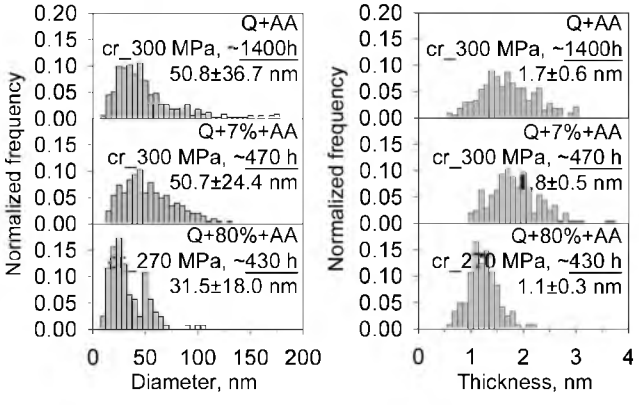


Fig. 4 Distribution of diameter and thickness of the Ω-phase plates within grains/subgrains after creep test to fracture at 150°C.

The main feature of microstructure evolution during creep is the formation of coarse film of Ω-phase along the deformation-induced boundaries (Fig. 3c and 3d). These films are composed of chains of fragmented plates of Ω-phase with average thickness of 4 nm (Fig. 3d). In addition, the precipitations of θ'-phase on crystallographic defects are observed under creep at 150°C. The main feature of dispersion of θ'-phase after creep test is the chain-like distribution for the sample without prior cold working and the uniform precipitation for the prior tensioned and/or rolled samples. It is

apparent, that increase in lattice dislocation density provides numerous nucleation sites for θ'-phase that facilitates their uniform precipitation.

Fracture surfaces of the prior cold deformed samples to strain of 0, 7, 80% after creep test at 150°C are shown in Fig. 5. The samples without prior cold deformation and the samples strained to 7% exhibit intergranular fracture, with the formation of very fine shallow dimples (Fig. 5a and b, respectively). On the other hand, the flat predominant tearing topography surface (TTS) having low macro roughness is observed in the sample subjected to extensive cold rolling (80%) (Fig. 5c). The TTS fracture does not exhibit evidence for sufficient plastic deformation before fracture (Fig. 2b). This fracture mode can be attributed to closely spaced microvoid nucleation and limited growth before coalescence, resulting in extremely shallow dimples [11]. We can assume that the boundary precipitation of Ω-phase plates facilitates the microcrack formation followed by their propagation along boundaries that leads to premature fracture under creep conditions.

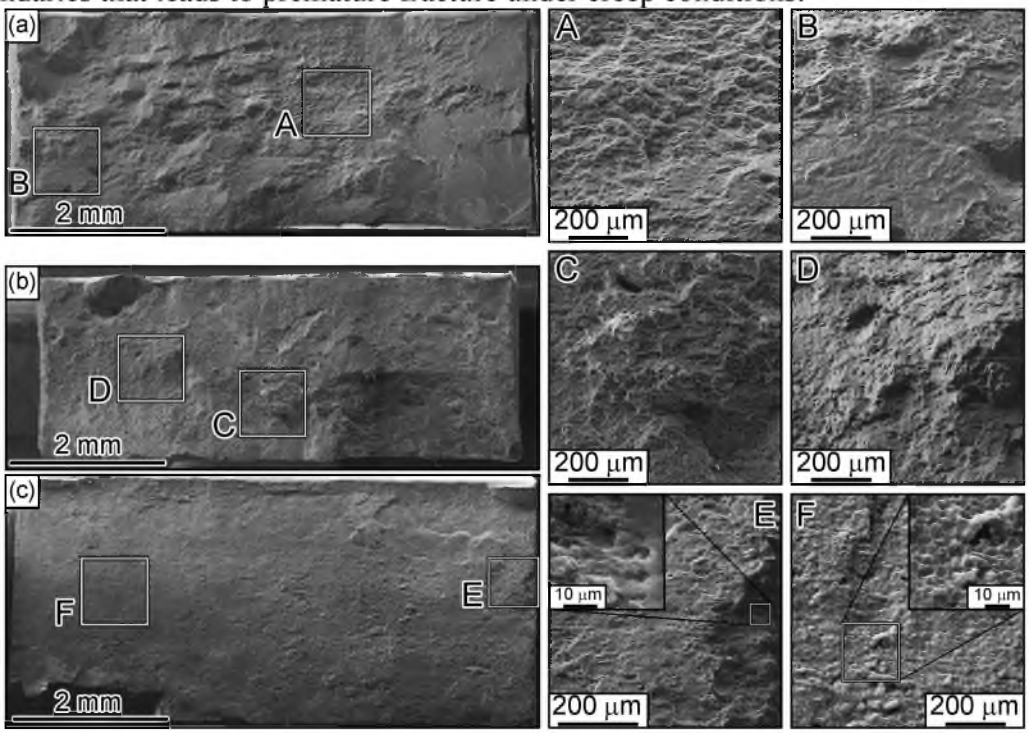


Fig. 5 Fracture surfaces of samples after creep test at 150°C and applied stress 300 MPa (a,b) and 270 MPa (c). Initial treatments: (a) quenching + ageing (190°C, 2 h), (b) tensioned (7%) + ageing (190°C, 2 h), (c)cold rolling (80%) + ageing (190°C, 2 h).

Thus, the increase in strength and the degradation of creep resistance of the samples subjected to prior cold deformation result from superposition of two competitive processes. First, an increase in lattice dislocation density facilitates precipitation of Ω-phase plates with high aspect ratio that leads to increment of static strength at room temperature. Minor increase in portion of θ′-phase is not important for increment in the YS. Perhaps, it is attributed to the fact that cold deformation provides uniform distribution of these particles. Second, an increase in lattice dislocation density accelerates diffusion processes during creep that results in coarsening of strengthening phase in grain/subgrain interiors and deteriorates creep resistance. It is obvious that the resistance of Ω-phase against coarsening depends on the dislocation density. The growth of Ω-phase plates during creep leads to decrease in the AR value that diminishes strength of the alloy. In addition, the precipitation of Ω-phase on deformation-induced boundaries facilitates intergranular fracture that decreases elongation-to-failure during creep. Therefore, the Al-Cu-Mg-Ag alloy subjected to TMP may be strong at room temperature or exhibits superior creep resistance at 150°C but these properties are rarely observed. It seems that the YS and UTS at room temperature and rupture time or minimal creep rate at 150°C are the key mechanical properties of this material but these properties are typically opposite to each other.

**Summary**

The effect of thermomechanical treatments including prior plastic deformation on the creep resistance of an Al-5.6Cu-0.72Mg-0.5Ag-0.32Mn-0.17Sc-0.12Zr (wt. %) alloy at 150°C was examined. Increasing the strain of plastic deformation prior to artificial aging leads to achieving high static mechanical properties and decrease of creep resistance, concurrently.

**Acknowledgements**

This study was supported by grant No. OK-591/0402-13. The authors are grateful to the staff of the Joint Research Center, Belgorod State University, for their assistance with the mechanical and structural characterizations.

**References**

[1]. I.J. Polmear, G. Pons, Y. Barbaux, H. Octor, C. Sanchez, A..J. Morton, W.E. Borbidge, S. Rogers, After Concorde: Evaluation of creep resistant Al-Cu-Mg-Ag alloys, Mater. Sci. Tech. 15 (1999) 861-868.

[2]. D. Bakavos, P.B. Prangnell, B. Bes, F. Eberl, The effect of silver on microstructural evolution in two 2xxx series Al-alloys with a high Cu:Mg ratio during ageing to a T8 temper, Mater. Sci. Eng. A491 (2008) 214-223.

[3]. M. Vural, J. Caro, Experimental analysis and constitutive modeling for the newly developed 2139-T8 alloy, Mater. Sci. Eng. A520 (2009) 56-65.

[4]. J. Wang, X. Wu, K. Xia, Creep behaviour at elevated temperatures of an Al-Cu-Mg-Ag alloy, Mater. Sci. Eng. A234-236 (1997) 287-290.

[5]. Y. Li, Z. Liu, S. Bai, X. Zhou, H. Wang, S. Zeng, Enhanced mechanical properties in an Al-Cu-Mg-Ag alloy by duplex aging, Mater. Sci. Eng. A528 (2011) 8060-8064.

[6]. M. Gazizov, V. Teleshov, V. Zakharov, R. Kaibyshev, Solidification behaviour and the effects of homogenisation on the structure of an Al-Cu-Mg-Ag-Sc alloy, J. Alloys Compd. 509 (2011) 9497-9507.

[7]. M. Gazizov, R. Kaibyshev, Effect of over-aging on the microstructural evolution in an Al-Cu-Mg-Ag alloy during ECAP at 300°C, J. Alloys Compd. 527 (2012) 163-175.

[8]. M. Gazizov, I. Zuiko, R. Kaibyshev, Effect of plastic deformation on a dispersion of omega-phase and mechanical properties of an Al-Cu-Mg-Ag alloy (Proceedings of International Conference THERMEC, Dec. 2-6, 2013, Las Vegas, USA)

[9]. J.F. Nie, B.C. Muddle, Microstructural design of high-strength aluminum alloys, J. Ph. Equilib. 19(6) (1998) 543-551

[10]. I.J. Polmear, G. Pons, H. Octor, C. Sanchez, A.J. Morton, W.E. Borbidge, S. Rogers, After Concorde: Evaluation of creep resistant Al-Cu-Mg-Ag alloy for use in the proposed European SST, Mater. Sci. Forum. 217-222 (1996) 1759-1764.

[11]. A.W. Thompson, J.C. Chesnutt, "Identification of a Fracture Mode: The Tearing Topography. Surface, Metall. Trans. A 10A (1979) 1193-1196.